

Design optimization of semi-rigid space steel frames with semi-rigid bases using biogeography-based optimization and genetic algorithms

Osman Shalla^{1a}, Hassan M. Maaly^{1b}, Merve Sagiroglu^{2c} and Osman Hamdy^{*1}

¹Department of Structural Engineering, University of Zagazig, Zagazig, Egypt
²Department of Civil Engineering, Technical University of Erzurum, Erzurum, Turkey

(Received November 22, 2018, Revised February 11, 2019, Accepted February 20, 2019)

Abstract. This paper performs for the first time a simultaneous optimization for members sections along with semi-rigid beam-to-column connections for space steel frames with fixed, semi-rigid, and hinged bases using a biogeography-based optimization algorithm (BBO) and a genetic algorithm (GA). Furthermore, a member's sections optimization for a fully fixed space frame is carried out. A real and accurate simulation of semi-rigid connection behavior is considered in this study, where the semi-rigid base connections are simulated using Kanvinde and Grilli (2012) nonlinear model, which considers deformations in different base connection components under the applied loads, while beam-to-column connections are modeled using the familiar Frye and Morris (1975) nonlinear polynomial model. Moreover, the P- Δ effect and geometric nonlinearity are considered. AISC-LRFD (2016) specification constraints of the stress and displacement are considered as well as section size fitting constraints. The optimization is applied to two benchmark space frame examples to inspect the effect of semi-rigidity on frame weight and drift using BBO and GA algorithms.

Keywords: genetic algorithm; biogeography-based optimization; semi-rigid space steel frame; optimization; semi-rigid base

1. Introduction

Beam-to-column connections along with base connections are usually assumed either a completely pinned or an entirely rigid connection. These two simplifying assumptions produce an incorrect estimation of the frame response. In fact, the steel connections are between these two severe assumptions and have some rotational stiffness; in addition, the real behavior of steel connection is complicated nonlinear, especially if the connection behavior is considered in the three dimensions in a space frame.

AISC-LRFD (2016) described two types of steel constructions: fully restrained (FR) and partially restrained (PR), where the PR type is considered according to reasonable experimental and numerical studies.

2. The studies of semi-rigid connection simulation

Some researchers worked on the behavior of semi-rigid

connections using experimental studies to obtain the nonlinear behavior of the connection such as Frye and Morris (1975), Abdalla and Chen (1995), Chisala (1999), Kim *et al.* (2010), Wu *et al.* (2012), Aydin *et al.* (2015), Maali *et al.* (2015), Aydın *et al.* (2015), Maali *et al.* (2016), Maali *et al.* (2017), Sağıroğlu *et al.* (2018), Maali *et al.* (2018). As a result of its wise simulation and its broad usage in the literature studies, the odd-polynomial Frye and Morris (1975) model are used in the current study.

On the other hand, developing an accurate model for semi-rigid base connections is usually unobserved in most of the literature studies. Merely Kanvinde and Grilli (2012) produce a rational model for simulating the semi-rigid base connection. This model takes into account the deformations of all different base connection elements, so it is used in this paper to simulate the base connections' behavior.

Table 1 presents a summary of the previous literature studies, where all the literature studies use the Frye and Morris (1975) model for modeling beam-to-column connections, in addition, Hensman and Nethercot (2001) model for simulating the base connection if the study considers the semi-rigid base connection.

3. Optimization algorithms

Two of the evolutionary population-based optimization algorithms are used in this paper, a biogeography-based optimization algorithm (BBO) and a genetic algorithm (GA). BBO is proposed by Dan Simon (2008), which imitates the colonization and extinction of species between

*Corresponding author, Ph.D. Student
E-mail: Osmanhmdy@gmail.com

^aProfessor and Head of Structural Department
E-mail: Osmanshalan@yahoo.com

^bAssociate Professor
E-mail: Dr.H.Maaly6@gmail.com

^cAssociate Professor
E-mail: merve.sagiroglu@erzurum.edu.tr

Table 1 Summary for the previous literature studies

Study	Frame	Base	Used algorithm	Design code
Shallan <i>et al.</i> (2018)	Plane	Semi-rigid	BA, GA	AISC-LRFD
Shallan <i>et al.</i> (2018)	Plane	Fixed	TLBO, GA	AISC-LRFD
Musa and Ayse (2016)	Space	Fixed	GA, HS	AISC-LRFD
Musa Artar (2016)	Plane	Fixed	TLBO	AISC-ASD
Musa and Ayse (2015)	Plane	Semi-rigid	GA	AISC-ASD
Musa and Ayse (2015)	Plane	Fixed	GA	AISC-LRFD
Musa and Ayse (2015)	Space	Fixed	GA	AISC-LRFD
Hadidi and Rafiee (2015)	Plane	Fixed	New HS	AISC-LRFD
Mohammad and Payam (2015)	Plane	Fixed	Fuzzy GA	AISC-ASD
Alqedra <i>et al.</i> (2015)	Plane	Fixed	ITHS	AISC-LRFD
Hadidi and Rafiee (2014)	Plane	Fixed	Improved PSO	AISC-LRFD
Rafiee and Hadidi (2013)	Plane	Fixed	BB-BC	AISC-LRFD
Arafa <i>et al.</i> (2011)	Plane	Fixed	HS	AISC-LRFD
Hayalioglu and Degertekin (2010)	Plane	Semi-rigid	HS	AISC-LRFD
Hayalioglu and Degertekin (2005)	Plane	Semi-rigid	GA	AISC-LRFD
Hayalioglu and Degertekin (2004)	Plane	Fixed	GA	AISC-ASD
Hayalioglu and Degertekin (2004)	Plane	Fixed	GA	Turkish code
Degertekin and Hayalioglu (2004)	Plane	Semi-rigid	GA	Turkish code

BA: Bees algorithm, ITHS: Intelligent tuned harmony search, TLBO: Teaching-learning-based optimization, HS: Harmony search, PSO: Particle swarm optimization, BB-BC: Big bang-big crunch

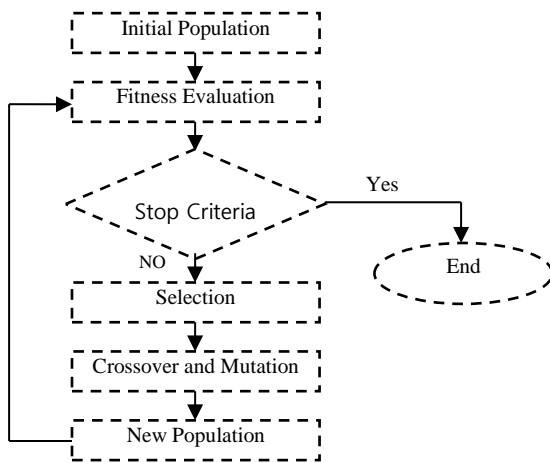


Fig. 1 Flowchart of the basic GA

islands. In addition, GA is inspired by John Holland, which simulates the evolution theory (Goldberg 1989).

3.1 Genetic algorithm (GA)

John Holland produced a genetic algorithm (Goldberg 1989), which is considered the mother of all evolutionary optimization algorithms. It simulates the evolution theory of Darwin. GA begins with an initial population composed of a certain number of listed chromosomes, where each chromosome represents a suggested solution to the problem. Each chromosome is made of a string of genes, where each

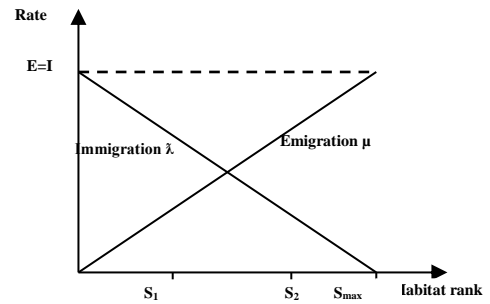


Fig. 2 The relationship between the rank of habitats S, emigration rate μ and immigration rate λ

gene signifies a particular suggested optimization variable. These genes are coded in a binary format; therefore, the decoding procedure is carried out to translate these genes into decimal values. These decimal values of the variables are used to solve the problem and determine the fitness value for each individual in the initial population. According to the fitness value of each chromosome, the selection step is performed to select the nominated chromosomes to go through a reproduction process. The main parameters of the reproduction process are crossover and mutation, which are used for constructing the next generation of suggested solutions. Then, the same steps are repeated until reaching the last generation. Fig. 1 shows a flowchart of the simple GA steps.

3.2 Biogeography-based optimization algorithm (BBO)

Biogeography-based optimization (BBO) is a population-based optimization technique inspired by Dan Simon (2008), where it mimics the colonization and extinction of the different species between the islands.

Same as GA, BBO starts with a certain number of islands or habitats forming the initial population. Each island represents a suggested solution for the problem and is characterized by a series of features called suitability index variables SIV, where each SIV represents a particular optimization variable.

Afterward, the habitat suitability index HSI of the problem is calculated for each habitat in the initial population, followed by sorting all habitats in accordance with the HSI values from the worst to the best. The worst solution has the highest HSI value and vice versa. After the sorting process, each habitat acquires a certain rank S, where S_{max} represents the total number of habitats in the population, that is to say, the population size.

In accordance with the habitat rank S, the modification parameters, immigration rate λ_s and emigration rate μ_s are determined using the following equations and as shown in Fig. 2.

$$\lambda_s = I \times \left(1 - \frac{S}{S_{max}}\right) \tag{1}$$

$$\mu_s = E \times \left(\frac{S}{S_{max}}\right) \tag{2}$$

Table 2 Comparison of the characteristics names for GA and BBO (Simon 2008)

GA	BBO
Gene	SIV
Chromosome	Habitat
Fitness	HSI
Reproduction	Modification
Crossover operator	Migration operator
Mutation operator	Mutation operator
Generation	Iteration

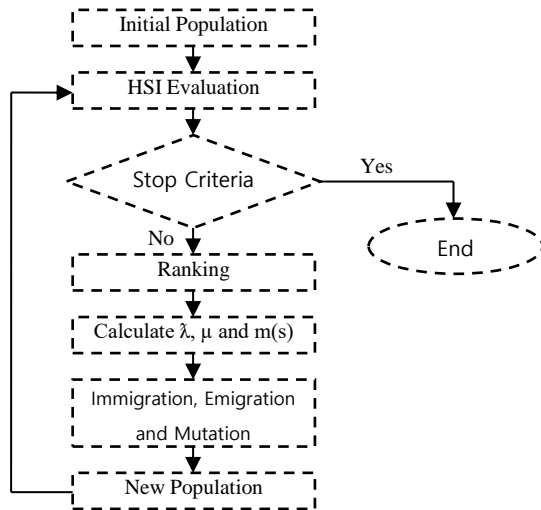


Fig. 3 Flowchart of the basic BBO algorithm

where I and E are the upper limits of possible immigration and emigration rates, in that order, generally for simplification are taken $I=E=1$.

Immigration indicates receiving new features, i.e., SIVs from good habitats, in contrast, emigration denotes sharing features of a good habitat with poor habitats. Hence, the habitat owns a high HSI possesses a lower rank S and a high immigration rate λ and a low emigration rate μ and contrariwise, where λ and μ limit from 0 to 1. A comparison between the names of GA and BBO characteristics is shown in Table 2.

Together with immigration and emigration procedures, the mutation process is carried out to increase the diversity of the population and to diminish the probability of getting trapped in local optima. Mutation in BBO means a random modification in a randomly selected variable, i.e., SIV, where mutation rate $m(s)$ can be determined as follows.

$$m(s) = m_{\max} \times \left[\frac{1 - P_s}{P_{\max}} \right] \quad (3)$$

where m_{\max} is a user-defined parameter, P_s is the probability of a habitat to have rank S , P_s is calculated based on λ_s and μ_s values based on Dan Simon (2008), and $P_{\max} = \max_S P_s$, $S=1, \dots, S_{\max}$.

The number of the elite is a user-defined number signifies the best habitats in the population will be

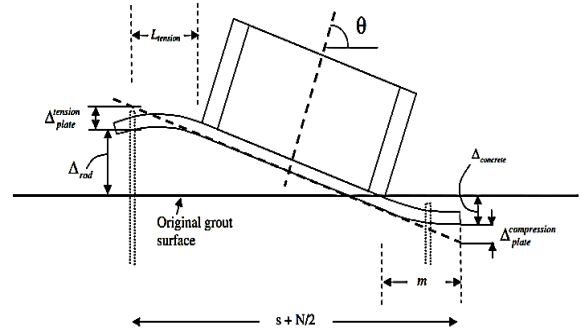


Fig. 4 Assumed deformation mode and contribution of various components Kanvinde and Grilli (2012)

excluded from the modification process to keep its good features to the next iteration.

By means of the three modification parameters, i.e., immigration, emigration, and mutation, the modification procedure is performed to modify the population. The modified population acts as a population for the next iteration, equivalent to the next generation in GA.

The previous steps are repeated until attainment of the final iteration and obtaining the most optimum solution throughout all the iterations as shown in Fig. 3.

4. Modeling of a semi-rigid base connection

For modeling the semi-rigid steel base connection, Kanvinde, Grilli and Zareian (2012) model is used in the current study. Kanvinde model is divided into two cases according to the eccentricity value e and critical eccentricity value e_{crit} .

A-condition 1, low-eccentricity case

In this condition, $e < e_{\text{crit}}$ and the spring rotation θ_r of the base connection is produced by concrete strain at the base plate edge $\epsilon_{\text{conc.}}^{\text{toe}}$ and concrete strain at the center of the anchor rods in the opposite side $\epsilon_{\text{conc.}}^{\text{rod}}$.

$$\theta_r = \frac{d \times (\epsilon_{\text{conc.}}^{\text{toe}} - \epsilon_{\text{conc.}}^{\text{rod}})}{(S + N/2)} \quad (4)$$

where d is the concrete depth under the base plate, and $(S + N/2)$ distance is shown in Fig. 4.

B- condition 2, high eccentricity case

In this condition, $e > e_{\text{crit}}$ and the spring rotation θ_r of the base connection is created by anchor strain Δ_{rod} . Due to a tensile force, concrete strain $\Delta_{\text{conc.}}$ and plate flap deformation on both compression side $\Delta_{\text{comp.}}$ and tension side $\Delta_{\text{ten.}}$. As shown in Fig. 4 and Eq. (5).

$$\theta_r = \frac{(\Delta_{\text{rod}} + \Delta_{\text{conc.}} + \Delta_{\text{ten.}} + \Delta_{\text{comp.}})}{(S + N/2)} \quad (5)$$

For simplification, some parameters are considered constant throughout the analysis process as follows: Rod gross diameter=2.5 cm, $d=70$ cm, two anchor rods are used with 50 cm length, plate thickness equals 2.5 cm, and the base plate extension out of column section=15 cm for each side, the pedestal extension out of the base

Table 3 The curve-fitting constants

Connection type	Curve-fitting constants		
	C ₁	C ₂	C ₃
1	4.28×10 ⁻³	1.45×10 ⁻⁹	1.51×10 ⁻¹⁶
2	3.66×10 ⁻⁴	1.15×10 ⁻⁶	4.57×10 ⁻⁸
3	2.23×10 ⁻⁵	1.85×10 ⁻⁸	3.19×10 ⁻¹²
4	8.46×10 ⁻⁴	1.01×10 ⁻⁴	1.24×10 ⁻⁸
5	1.83×10 ⁻³	1.04×10 ⁻⁴	6.38×10 ⁻⁶
6	1.79×10 ⁻³	1.76×10 ⁻⁴	2.04×10 ⁻⁴
7	2.10×10 ⁻⁴	6.20×10 ⁻⁶	-7.60×10 ⁻⁹
8	5.10×10 ⁻⁵	6.20×10 ⁻¹⁰	2.40×10 ⁻¹³

Table 4 The standardization parameter (κ)

Connection type	Standardization parameter (κ)
1	$\kappa = d_a^{-2.4} t_a^{-1.81} g^{0.15}$
2	$\kappa = d_a^{-2.4} t_a^{-1.81} g^{0.15}$
3	$\kappa = d^{-1.287} t^{-1.128} t_c^{-0.415} \rho_a^{-0.694} g^{1.35}$
4	$\kappa = d^{-1.5} t^{-0.5} \rho_a^{-0.7} d_b^{-1.5}$
5	$\kappa = d_g^{-2.4} t_p^{-0.4} d_b^{-1.5}$
6	$\kappa = d_g^{-2.4} t_p^{-0.6}$
7	$\kappa = d^{-1.5} t^{-0.5} \rho_t^{-0.7} d_b^{-1.1}$
8	$\kappa = d_p^{-2.3} t_p^{-1.6} t_w^{-0.5} g^{1.6}$

Table 5 The fixed connection size parameters

Connection type	Fixed connection size parameters (cm)
1	$t_a = 2.54, g = 11.43$
2	$t_a = 2.858, g = 25.4$
3	$t = 2.54, t_c = 2.54, g = 11.43$
4	$t = 2.54, d_b = 2.858$
5	$t_p = 2.54, d_b = 2.858$
6	$t_p = 2.54$
7	$t = 3.81, d_b = 2.858$
8	$t_p = 2.54, g = 25.4$

plate=10 cm for each side.

5. Modeling of a semi-rigid beam-to-column connection

Frye and Morris (1975) model is used in the current paper for simulating semi-rigid beam-to-column connections. In addition to its easiness to apply, it is an odd-power polynomial model, which is rationally reliable for modeling the nonlinear $M-\theta_r$ behavior of the semi-rigid connections, as expressed in the following equation.

$$\theta_r = C_1(\kappa M)^1 + C_2(\kappa M)^3 + C_3(\kappa M)^5 \quad (6)$$

where C₁, C₂, and C₃ are the curve-fitting constants, and κ is a standardization constant dependent on the connection type and its geometry, as shown in Tables 3 and 4 (Dhillon and O'Malley III 1999).

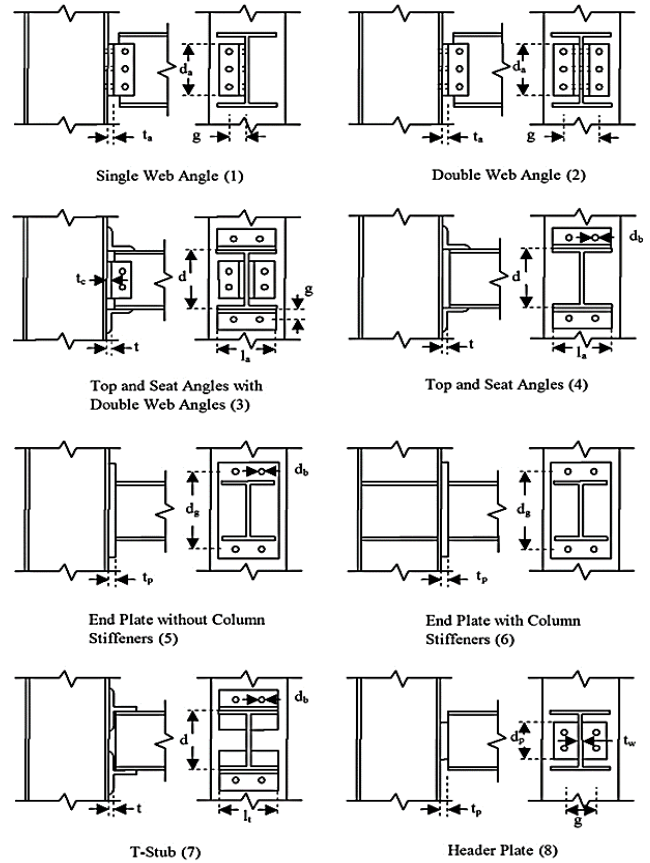


Fig. 5 Semi-rigid beam-to-column connection types (Hadidi and Rafiee 2015)

Fig. 5 reveals that Frye and Morris's model is valid for eight different types of semi-rigid beam-to-column connections and Fig. 6 shows the moment-rotation curves for the eight connections.

Following the literature studies (Hadidi and Rafiee 2014), (Hadidi and Rafiee 2015) and others, and for simplification, some of the connection size parameters are taken constantly throughout the analysis procedure, as shown in Table 5. Furthermore, for connections 1, 2, and 8, d_a & d_p =web depth-10.16 cm, and for connections 5 and 6, d_g =beam depth+15.24 cm (Shallan *et al.* 2018).

After determining the relative rotation of semi-rigid connection Θ_r , the relative rotational stiffness K of a semi-rigid connection will be determined using the following equations.

$$K_A = \frac{M_A}{\theta_{rA}} \quad K_B = \frac{M_B}{\theta_{rB}} \quad (7)$$

where A and B represent the A and B ends of a member.

6. Nonlinear analysis process using the stiffness method for a space frame

Stiffness method is an effective way to analyze complex structures. The stiffness matrix [K] for a fully rigid space member as shown in Fig. 7 such as a column with a fixed base is as follows, where 1, 2, and 3 imply X, Y, and Z axis, respectively.

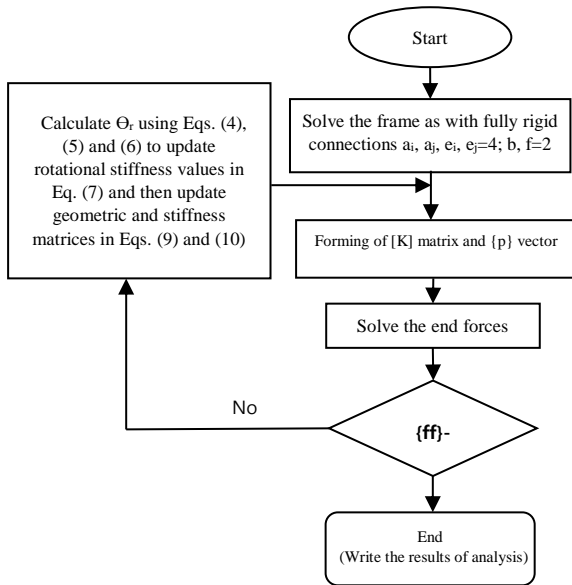


Fig. 8 Analysis procedure (Sagiroglu and Aydin 2015)

Table 6 A comparison between Artar and Daloglu (2016) and the current study

Items	Artar and Daloglu (2016)	Current study
Algorithms	GA & HS	GA & BBO
Program used	Sap 2000	Matlab
Analysis method	FEM	Stiffness method
No. of available semi-rigid connections	6	8
Connection stiffness	Constant	Nonlinear
Base case	Fixed	Fixed & semi-rigid & Hinged
Section optimization	Yes	Yes
Connection optimization	No	Yes
P-Δ effect	No	Yes
Geometric nonlinearity	No	Yes

FEM: Finite element method

nonlinearity as summarized in Fig. 8.

Table 6 shows a comparison between the current study and the literature study, Artar and Daloglu (2016), which performs a space frame optimization with semi-rigid beam-to-column connections. As shown in the table, Artar and Daloglu (2016) study considers the semi-rigidity of beam-to-column connections by assuming a constant rotational value for each connection type instead of considering the nonlinearity, that because of using Sap2000 (Habibullah 2013) to perform a linear analysis.

7. Optimization formulation

The algorithms used in the following numerical examples are genetic and biogeography-based optimization algorithms. The used parameters for GA are 0.9 for the uniform crossover and 0.05 for the mutation. While the used parameters for BBO are 1 for I and E, and elite ratio=20% of the population size. Both of the algorithms

have a population size of 100, and maximum generations/iterations of 50. The design variables, objective function and design constrains are as follows.

Design variable

Design variable is members cross-section selected among 64 available cross-sections for each member, and connection types selected among eight available connections shown in Fig. 5.

Objective function

The total weight of the steel frame is determined as follows.

$$W = \sum_{i=1}^{NM} \gamma_s A_i L_i \quad (22)$$

where γ_s is the steel density, A_i is the cross-sectional area, L_i is the member length, NM represents the total number of members.

The objective function $F(x)$ is expressed in the following equation.

$$F(x) = \frac{1}{W(1000C + 1)} \quad (23)$$

where C is the penalty coefficient equals zero for the solutions achieve all constraints, or else, it equals one.

Design constraints

To confirm that the resulted optimum frame is safe and usable, the following constraints are used in the current study.

1. AISC-LRFD (2016) strength constraint using the interaction equation of the bending moment and the axial force as shown in the following equations

$$\text{For } \frac{P_u}{\phi P_n} \geq 0.2 \left(\frac{P_u}{\phi P_n} \right) + \frac{8}{9} \left(\frac{M_{uz}}{\phi_b M_{nz}} + \frac{M_{uy}}{\phi_b M_{ny}} \right) \leq 1 \quad (24)$$

$$\text{For } \frac{P_u}{\phi P_n} < 0.2 \quad \frac{1}{2} \left(\frac{P_u}{\phi P_n} \right) + \left(\frac{M_{uz}}{\phi_b M_{nz}} + \frac{M_{uy}}{\phi_b M_{ny}} \right) \leq 1 \quad (25)$$

where P_u and P_n are the required and the nominal strength of a member, respectively, and ϕ is a reduction factor equals 0.9. Furthermore, M_{uz} and M_{uy} are the required flexural strengths of a member about the Z&Y axis, respectively. Also, M_{nz} and M_{ny} are the nominal flexural strengths of a member about the Z&Y axis, respectively, where the bending reduction factor ϕ_b equals 0.9.

2. Moreover, the roof drift and inter-story drift constraints are taken into account, where the allowable roof drift equals frame height/400. And the allowable inter-story drift is measured by story height/400.

3. Due to construction requirement, the size fitting constraint is considered by preventing a column depth or area on a higher floor to be bigger than the same column depth or area on a lower floor.

8. Numerical examples

Using BBO and GA optimization techniques, two benchmark examples are investigated in this paper, where

Table 7 Member sections and connections of optimum frames resulted by BBO

Group members	FF		SF		SS		SH	
	Sections	Sections	Connections	Sections	Connections	Sections	Connections	
1	W14X38	W16X36	-	W14X38	-	W24X68	-	
2	W12X19	W14X26	1	W18X35	7	W27X94	2	
3	W18X35	W18X35	5	W10X22	5	W12X19	1	

Table 8 Member sections and connections of optimum frames resulted by GA

Group members	FF		SF		SS		SH	
	Sections	Sections	Connections	Sections	Connections	Sections	Connections	
1	W16X40	W16X36	-	W16X36	-	W24X68	-	
2	W12X19	W16X26	1	W16X40	7	W27X94	5	
3	W16X31	W18X35	7	W12X19	3	W8X15	7	

simultaneous cross sections and beam-to-column connections optimization are carried out using Frye and Morris (1975) model and Kanvinde (2012) model. Four cases of steel frame are considered; (1) fully fixed FF (2) semi-rigid beam-to-column connections with fixed base SF (3) semi-rigid beam-to-column connections with semi-rigid bases SS (4) semi-rigid beam-to-column connections with hinged bases SH. The properties of the used steel, and available sections are as follows.

Steel properties

The properties of the used steel are: $E = 200$ GPa, yield stress $f_y = 250$ MPa, shear modulus $G = 77.2$ GPa, and the unit weight of material $\gamma_s = 7.85$ t/m², based on AISC-LRFD (2016).

Available sections

According to Artar and Daloglu (2016), 64 cross sections are available from W8x15 to W40x183.

8.1 Two stories, 16-member steel space frame

The first example is two stories, 16-member steel space frame, this example is optimized as a fully fixed frame and as a semi-rigid frame with fixed bases by Artar and Daloglu (2016).

The geometry, wind loads, and member grouping are shown in Fig. 9. In addition the vertical load on all beams is 20 kN/m, whereas, the allowable roof drift and inter-story drift are 1.8 cm and 0.9 cm, respectively.

Tables 7 and 8 show the member cross-sections and story connections for the optimum solutions using BBO and GA, respectively, for the four frame cases.

Moreover, the roof drift, inter-story drift and total frame weight of the optimum frames in this study are compared with those in previous studies in Table 9. The comparison shows that GA achieves better results than BBO for the four frame cases. Besides, the stiffest connection type 7 is usually selected.

Figs. 10 and 11 show the effect of the four frame cases on the roof drift and the weight, respectively, where these figures show that FF case results in the lightest frame

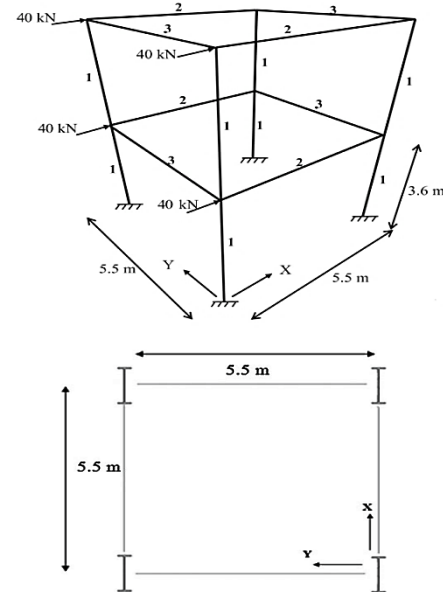


Fig. 9 Two stories, 16-member steel space frame (Artar and Daloglu 2016)

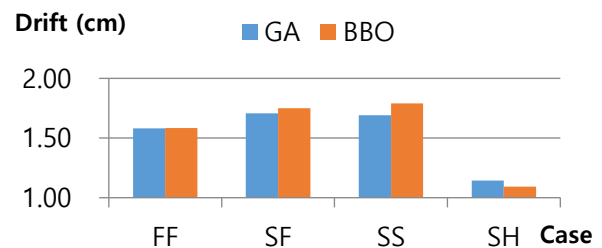


Fig. 10 The roof drift using BBO and GA

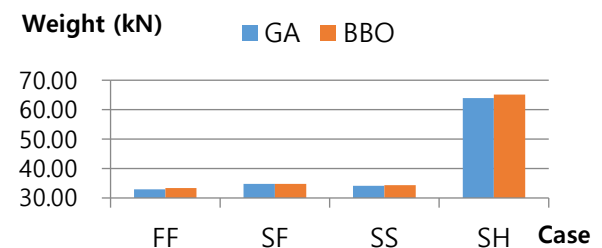


Fig. 11 The total frame weight using BBO and GA

followed by SS case then the SF case, while SH case results in the heaviest frame. Moreover, and unpredictably, SH results in the smallest roof drift.

The same study is carried out using GA but without considering the inter-story drift constraint. Table 10 shows the member cross-sections, story connections, roof drift, inter-story drift and frame weight for the optimum solutions using GA for the four frame cases without considering the inter-story drift constraint.

Moreover, Figs. 12 and 13 show the effect of the four frame cases on the roof drift and the weight, respectively.

Similar to previous results these figures show that FF case results in the lightest frame followed by SS and SF cases, while SH case results in the heaviest frame.

Table 9 Comparisons between the current study and previous works

Study	Algorithm	Case	Conn. type	R.d (cm)	In.d (cm)	W(kN)
Artar and Daloglu (2016)	GA	FF	—	1.63	0.85	37.68
		SF	2	1.41	0.57	41.94
		SF	3	1.48	0.58	40.67
		SF	4	1.38	0.59	39.40
		SF	5	1.66	0.86	39.32
		SF	6	1.46	0.62	37.79
		SF	7	1.72	0.88	37.68
Current study	GA	FF	—	1.58	0.82	33.37
		SF	O	1.75	0.90	34.83
		SS	O	1.79	0.90	34.38
		SH	O	1.09	0.78	65.13
		FF	—	1.58	0.83	32.95
		SF	O	1.71	0.87	34.82
		SS	O	1.69	0.86	34.15
		SH	O	1.14	0.81	63.89

R.d: Roof drift, In.d: Inter-story drift, W: Weight, O: Optimized, i.e/, optimized as shown in Tables 7 and 8

Table 10 Properties of the optimum frames resulted by GA without considering the inter-story drift constraint

Group members	FF		SF		SS		SH	
	Sections	Sections	Connections	Sections	Connections	Sections	Connections	
1	W16X40	W16X36	-	W16X36	-	W21X50	-	
2	W12X19	W12X19	1	W18X35	7	W24X68	7	
3	W16X26	W18X35	7	W12X19	1	W12X19	7	
R.d (cm)	1.77	1.71		1.73		1.80		
In.d (cm)	0.95	0.87		0.87		1.32		
W(kN)	31.37	32.51		32.51		49.09		

Drift (cm)

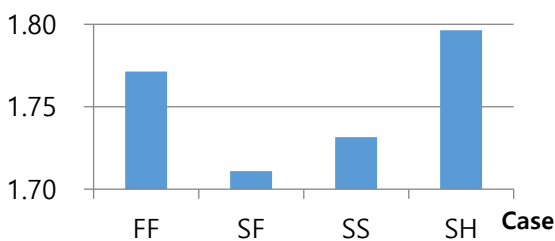


Fig. 12 The roof drift using GA

Weight (kN)



Fig. 13 The total frame weight using GA

Table 11 Gravity loads on the beams

Beams	Uniformly distributed load (kN/m)	
	Outer beams	Inner beams
Roof beams	7.38	14.77
Floor beams	10.72	21.44

Table 12 Wind loads on the external beams

Floor no.	Windward (kN/m)	Leeward (kN/m)
1	1.64	1.86
2	1.88	1.86
3	2.10	1.86
4	2.29	1.86
5	2.44	1.86
6	2.57	1.86
7	2.69	1.86
8	2.79	1.86
9	2.89	1.86
10	1.49	1.86

Contrarily to previous results, SH results in the largest roof drift and inter-story drift also which mightily violates the inter-story-drift constraint.

8.2 Ten stories, 568-member steel space frame

The Second example is ten stories, 568-member steel space frame, this example is optimized as a fully fixed frame by Hasançebi *et al.* (2010), Kaveh and Talatahari (2012) and Aydođu and Saka (2012). And optimized as a semi-rigid frame with fixed bases by Artar and Daloglu (2016). The geometry and members grouping are shown in Fig. 14.

Tables 11 and 12 show the gravity and wind loads, respectively, where two load cases are considered, wind loads at X direction then in Y direction.

The member cross-sections and story connections for the current optimum solutions using BBO and GA for the four frame cases are shown in Tables 13 and 14, respectively.

The allowable roof drift and inter-story drift are 9.14 cm and 0.914 cm, respectively.

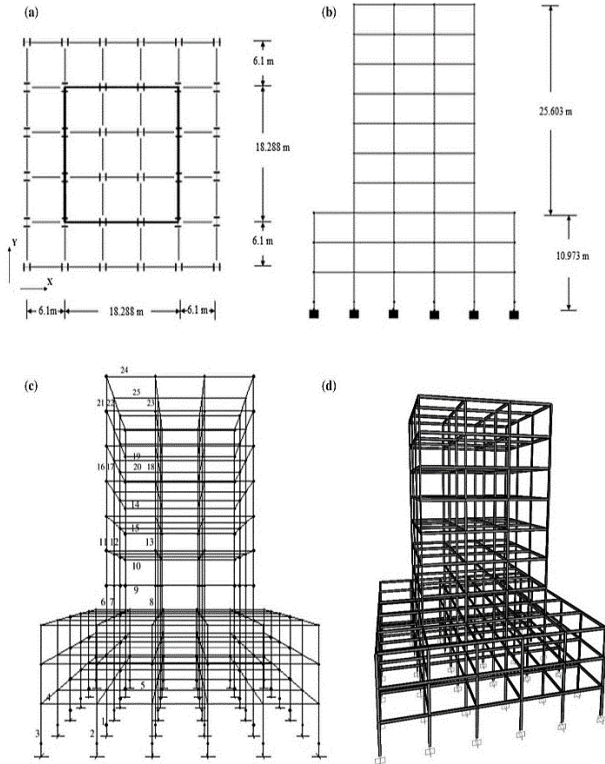


Fig. 14 Ten stories, 568-Member steel space frames, (a) Plan view, (b) Elevation, (c) Member grouping, (d) 3D view. Asterisks first group: inner column, second group: side columns, third group: corner columns, fourth group: outer beams, fifth group: inner beams and so forth (Artar and Daloglu 2016)

Furthermore, the roof drift, inter-story drift and total frame weight of the optimum frames in the current study are compared with those in previous studies in Table 15. Similar to the first example result, GA achieves better results than BBO for the four frame cases.

In addition, the stiffest connections types 7, 6, and 5 are usually selected, while the most flexible type 1 is usually selected for the roof floor.

Figs. 15 and 16 show the influence of the four frame cases on the roof drift and the weight, respectively, where these figures show that FF case results in the lightest frame followed by SS case then the SF case, while SH case results in the heaviest frame. Furthermore, SH results in largest roof drift, where the lower floors in this frame are highly controlled by strength constraint more than other constraints due to its weight.

9. Conclusions

Actual simulation of semi-rigid steel connections is very important to achieve accurate results for the frame analysis. This study attempts to perform optimization for fully fixed and semi-rigid frames, whereas beam-to-column and base connections are simulated using logically Frye and Morris (1975) and Kanvinde (2012) models, respectively. The current study is carried out to two benchmark problems

Table 13 Member sections and connections of optimum frames resulted by BBO

Group members	FF		SF		SS		SH	
	Sections	Sections	Connections	Sections	Connections	Sections	Connections	
1	W40X149	W40X183	-	W40X183	-	W40X183	-	
2	W10X33	W14X34	-	W12X30	-	W14X43	-	
3	W12X26	W8X21	-	W8X21	-	W10X22	-	
4	W8X21	W8X28	3	W8X28	3	W10X22	6	
5	W21X50	W18X35	7	W18X35	7	W24X68	7	
6	W16X36	W14X38	-	W14X38	-	W21X62	-	
7	W24X68	W30X108	-	W30X108	-	W24X68	-	
8	W40X149	W30X108	-	W30X108	-	W40X149	-	
9	W18X35	W18X50	2	W18X76	2	W18X35	6	
10	W18X40	W18X76	7	W18X50	7	W18X40	7	
11	W16X36	W14X38	-	W14X38	-	W21X62	-	
12	W24X68	W30X108	-	W30X108	-	W24X68	-	
13	W40X149	W30X108	-	W30X108	-	W40X149	-	
14	W16X36	W16X36	2	W16X36	2	W18X50	7	
15	W14X30	W14X53	5	W14X53	5	W14X34	5	
16	W16X36	W14X38	-	W14X38	-	W14X61	-	
17	W24X68	W30X108	-	W30X108	-	W24X68	-	
18	W40X149	W30X108	-	W30X108	-	W40X149	-	
19	W12X26	W16X36	7	W16X36	7	W14X30	5	
20	W16X31	W14X34	5	W14X34	5	W18X35	5	
21	W8X15	W14X38	-	W14X38	-	W10X33	-	
22	W14X26	W30X108	-	W30X108	-	W14X38	-	
23	W12X26	W30X108	-	W30X108	-	W24X68	-	
24	W8X21	W24X68	4	W24X68	4	W14X26	2	
25	W14X30	W14X34	1	W14X34	1	W12X30	1	

Table 14 Member sections and connections of optimum frames resulted by GA

Group members	FF		SF		SS		SH	
	Sections	Sections	Connections	Sections	Connections	Sections	Connections	
1	W36X150	W40X183	-	W40X183	-	W40X183	-	
2	W8X28	W14X34	-	W12X30	-	W14X43	-	
3	W16X26	W8X21	-	W8X21	-	W10X22	-	
4	W8X24	W8X28	3	W8X28	3	W10X22	6	
5	W18X35	W18X35	7	W18X35	7	W24X68	7	
6	W18X50	W14X38	-	W14X38	-	W21X62	-	
7	W24X68	W30X108	-	W30X108	-	W24X68	-	
8	W36X150	W30X108	-	W30X108	-	W40X149	-	
9	W21X50	W18X76	2	W18X50	2	W18X35	6	
10	W14X30	W18X50	7	W18X76	7	W18X40	7	
11	W18X50	W14X38	-	W14X38	-	W21X62	-	
12	W24X68	W30X108	-	W30X108	-	W24X68	-	
13	W36X150	W30X108	-	W30X108	-	W40X149	-	
14	W14X30	W16X36	2	W16X36	2	W18X50	7	
15	W14X30	W14X53	5	W14X43	5	W14X34	5	

Table 14 Continued

16	W12X26	W14X38	-	W14X38	-	W14X61	-
17	W24X68	W30X108	-	W30X108	-	W24X68	-
18	W36X150	W30X108	-	W30X108	-	W40X149	-
19	W16X26	W8X35	7	W10X22	7	W14X30	5
20	W10X26	W14X34	5	W14X34	5	W18X35	5
21	W10X15	W14X38	-	W14X38	-	W10X22	-
22	W24X68	W30X108	-	W30X108	-	W14X43	-
23	W8X24	W30X108	-	W30X108	-	W14X61	-
24	W8X21	W24X68	4	W24X68	4	W14X26	4
25	W16X26	W14X34	1	W14X34	1	W14X30	1

Table 15 Comparisons between the current study and previous works

Study	Algorithm	Case	Conn. type	R.d (cm)	In.d (cm)	W (kN)
Hasançebi <i>et al.</i> (2010)	TSO	FF	-	-	-	2,307
Kaveh and Talatahari (2012)	PSO	FF	-	-	-	2,369
Aydodu and Saka (2012)	ACO	FF	-	-	-	2,242
Artar and Daloglu (2016)	GA	FF	-	7.14	0.91	1,987
		SF	2	7.83	0.91	2,252
		SF	3	7.43	0.91	2,735
		SF	4	7.81	0.89	2,498
		SF	5	7.22	0.86	2,454
		SF	6	7.05	0.91	2,339
		SF	7	7.15	0.91	2,324
	HS	FF	-	7.86	0.91	2,109
		SF	2	7.76	0.91	2,537
		SF	3	7.91	0.91	2,505
		SF	4	7.30	0.90	2,290
		SF	5	7.40	0.91	2,275
		SF	6	7.00	0.91	2,315
		SF	7	7.18	0.91	2,177
Current study	BBO	FF	-	7.08	0.91	2,041
		SF	0	6.85	0.91	2,349
		SS	0	7.20	0.91	2,339
	GA	SH	0	8.24	0.91	2,460
		FF	-	5.77	0.79	1,898
		SF	0	7.32	0.91	2,347
		SS	0	7.20	0.91	2,287
		SH	0	8.15	0.91	2,459

TSO: Technology Selection and Operation, ACO: Ant colony optimization

using BBO and GA algorithms and the following results are found.

- Fully fixed frame FF case result in the lightest frame, along with a relatively small roof drift.
- The SH case result in the heaviest frame and the largest roof drift.
- On the other hand, if the frame is highly controlled by

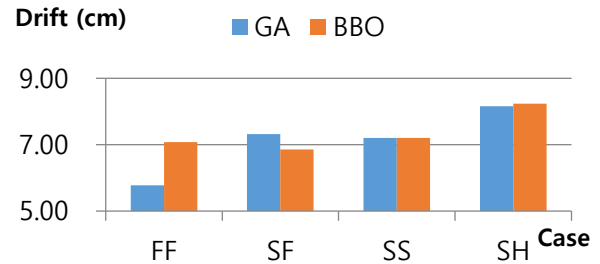


Fig. 15 The roof drift using BBO and GA

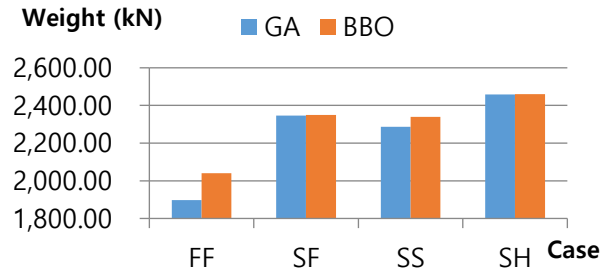


Fig. 16 The total frame weight using BBO and GA

inter-story drift constraint more than other constraints such in small frames, the SH will result in the smallest roof drift.

• Furthermore, the stiffest connections types are usually selected for most of the floors except higher floors where the most flexible connections are selected.

• GA achieves better results than BBO for all examples and for all frame cases.

References

- Abdalla, K.M. and Chen, W.F. (1995), "Expanded database of semi-rigid steel connections", *Comput. Struct.*, **56**(4), 553-564.
- Alqedra, M., Khalifa, A. and Arafa, M. (2015), "An intelligent tuned harmony search algorithm for optimum design of steel framed structures to AISC-LRFD", *Adv. Res.*, **4**(6), 421-40.
- American Institute of Steel Construction (2016), *ANSI/AISC 360-16. Specification for Structural Steel Buildings*, American Institute of Steel Construction.
- Arafa, M., Khalifa, A. and Alqedra, M. (2011), "Design optimization of semi-rigidly connected steel frames using harmony search algorithm", M.Sc. Dissertation, Gaza University, Palestine.
- Artar, M. (2016), "Optimum design of braced steel frames via teaching learning based optimization", *Struct. Eng. Mech.*, **22**(4), 733-744.
- Artar, M. and Daloglu, A.T. (2015), "Optimum design of steel space frames with composite beams using genetic algorithm", *Steel Compos. Struct.*, **19**(2), 503-519.
- Artar, M. and Daloglu, A.T. (2016), "Optimum weight design of steel space frames with semi-rigid connections using harmony search and genetic algorithms", *Neur. Comput. Appl.*, **29**(11), 1089-1100.
- Artar, M. and Dalolou, A.T. (2015), "Optimum design of composite steel frames with semi-rigid connections and column bases via genetic algorithm", *Steel Compos. Struct.*, **19**(4), 1035-1053.
- Aydin, A.C., Kiliç, M., Maali, M. and Sağıroğlu, M. (2015),

- “Experimental assessment of the semi-rigid connections behavior with angles and stiffeners”, *J. Constr. Steel Res.*, **114**, 338-348.
- Aydın, A.C., Maali, M., Kılıç, M. and Sağiroğlu, M. (2015), “Experimental investigation of sinus beams with end-plate connections”, *Thin-Wall. Struct.*, **97**, 35-43.
- Aydodu, I. and Saka, M.P. (2012), “Ant colony optimization of irregular steel frames including elemental warping effect”, *Adv. Eng. Softw.*, **44**(1), 150-169.
- Chisala, M.L. (1999), “Modelling M- ϕ curves for standard beam-to-column connections”, *Eng. Struct.*, **21**(12), 1066-1075
- Degertekin, S.O. and Hayalioglu, M.S. (2010), “Harmony search algorithm for minimum cost design of steel frames with Semi-rigid connections and column bases”, *Struct. Multidiscipl. Optim.*, **42**(5), 755-768.
- Degertekin, S.O. and Hayalioglu, M.S. (2004), “Design of non-linear semi-rigid steel frames with semi-rigid column bases”, *Electr. J. Struct. Eng.*, **4**(10), 1-16.
- Dhillon, B.S. and O'Malley III, J.W. (1999), “Interactive design of semirigid steel frames”, *J. Struct. Eng.*, **125**(5), 556-564.
- Frye, M.J. and Morris, G.A. (1975), “Analysis of flexibly connected steel frames”, *Can. J. Civil Eng.*, **2**(3), 280-291.
- Goldberg, D.E. (1989), *Genetic Algorithms in Search, Optimization, and Machine Learning*, Addison Wesley.
- Habibullah, A. (2013), *SAP2000*, CSI Knowledge Base.
- Hadidi, A. and Rafiee, A. (2014), “Harmony search based, improved particle swarm optimizer for minimum cost design of semi-rigid steel frames”, *Struct. Eng. Mech.*, **50**(3), 323-347.
- Hadidi, A. and Rafiee, A. (2015), “A new hybrid algorithm for simultaneous size and semi-rigid connection type Optimization of steel frames”, *Int. J. Steel Struct.*, **15**(1), 89-102.
- Hasançebi, O., Çarbaş, S., Doğan, E., Erdal, F. and Saka, M.P. (2010), “Comparison of non-deterministic search techniques in the optimum design of real size steel frames”, *Comput. Struct.*, **88**(17-18), 1033-1048.
- Hayalioglu, M.S. and Degertekin, S.O. (2004), “Design of non-linear steel frames for stress and displacement constraints with semi-rigid connections via genetic optimization”, *Struct. Multidiscipl. Optim.*, **27**(4), 259-271.
- Hayalioglu, M.S. and Degertekin, S.O. (2005), “Minimum cost design of steel frames with semi-rigid connections and column bases via genetic optimization”, *Comput. Struct.*, **83**(21-22), 1849-1863.
- Hensman, J.S. and Nethercot, D.A. (2001), “Numerical study of unbraced composite frames: Generation of data to validate Use of the wind moment method of design”, *J. Constr. Steel Res.*, **57**(7), 791-809.
- Kanvinde, A.M., Grilli, D.A. and Zareian, F. (2012), “Rotational stiffness of exposed column base connections: Experiments and analytical models”, *J. Struct. Eng.*, **138**(5), 549-560.
- Kaveh, A. and Talatahari, S. (2012), “A hybrid CSS and PSO algorithm for optimal design of structures”, *Struct. Eng. Mech.*, **42**(6), 783-797.
- Kim, J.H., Ghaboussi, J. and Elnashai, A.S. (2010), “Mechanical and informational modeling of steel beam-to-column connections”, *Eng. Struct.*, **32**(2), 449-458.
- Maali, M., Aydın, A.C. and Sağiroglu, M. (2015), “Investigation of innovative steel runway beam in industrial building”, *Sadhan.* **40**(7), 2239-2251.
- Maali, M., Kılıç, M. and Aydın, A.C. (2016), “Experimental model of the behaviour of boltedangles connections with stiffeners”, *Int. J. Steel Struct.*, **16**(3), 719-733.
- Maali, M., Kılıç, M., Sağiroğlu, M. and Aydın, A.C. (2017), “Experimental model for predicting the semi-rigid connections’ behaviour with angles and stiffeners”, *Adv. Struct. Engineering* **20**(6), 884-95.
- Maali, M., Sağiroglu, M. and Solak, M.S. (2018), “Experimental behavior of screwed beam-to-column connections in cold-formed steel frames”, *Arab. J. Geosci.*, **11**(9), 205.
- Rafiee, A., Talatahari, S. and Hadidi, A. (2013), “Optimum design of steel frames with semi-rigid connections using big bang-big crunch method”, *Steel Compos. Struct.*, **14**(5), 431-451.
- Sagiroglu, M. and Aydın, A.C. (2015), “Design and analysis of non-linear space frames with semi-rigid connections”, *Steel Compos. Struct.*, **18**(6), 1405-1421.
- Sağiroğlu, M., Maali, M., Kılıç, M. and Aydın, A.C. (2018), “A novel approach for bolted T-stub connections”, *Int. J. Steel Struct.*, **18**(3), 891-909.
- Sedat, M., Degertekin, S. and Gorgun, H. (2004), “Design of semi-rigid planar steel frames according to Turkish steel design code”, *J. Eng. Nat. Sci.*, **412**, 101-116.
- Shallan, O., Hassan, M.M. and Hamdy, O. (2018), “Simultaneous design optimization of semi-rigid plane steel frames with semi-rigid bases using bees and genetic algorithms”, *Int. J. Eng. Technol.*, **10**(6), 1641-1660.
- Shallan, O., Hassan, M.M. and Hamdy, O. (2018), “A developed design optimization model for semi-rigid steel frames using teaching-learning-based optimization and genetic algorithms”, *Struct. Eng. Mech.*, **66**(2), 173-183.
- Simon, D. (2008), “Biogeography-based optimization”, *IEEE Trans. Evolut. Comput.*, **12**(6), 702-713.
- Wu, Z., Zhang, S. and Jiang, S.F. (2012), “Simulation of tensile bolts in finite element modeling of semi-rigid beam-to-column connections.” *Int. J. Steel Struct.*, **12**(3), 339-350.
- Yassami, M. and Ashtari, P. (2015), “Using fuzzy genetic algorithm for the weight optimization of steel frames with semi-rigid connections”, *Int. J. Steel Struct.*, **15**(1), 63-73.

CC